Article:
Baylay, J., Thornber, T. and Lidzey, D.G. (2026) Characterising power generation by model photovoltaic towers located in a simulated urban environment. Energies, 19 (4). 1077. ISSN: 1996-1073

https://doi.org/10.3390/en19041077

energies

MDPI

Article

Characterising Power Generation by Model Photovoltaic Towers Located in a Simulated Urban Environment

Joseph Baylay, Timothy Thornber and David G. Lidzey *

School of Mathematical and Physical Sciences, The University of Sheffield, Hicks Building, Hounsfield Road, Sheffield S3 7RH, UK; joe.baylay@gmail.com (J.B.); tthornber1@sheffield.ac.uk (T.T.)
* Correspondence: d.g.lidzey@sheffield.ac.uk

Abstract

Solar cell installations are most often located in places where there is abundant open space. It is however more difficult to place solar cells in urban environments due to space constraints and suboptimal light conditions. One potential solution is to create three-dimensional structures covered with solar cell modules having a relatively small physical footprint (e.g., with a shape such as a tower), creating a three-dimensional (3D) solar cell installation (sometimes called 'power towers'). To explore this, we fabricate physical models of 3D towers covered with solar cells (here referred to as 3DPV towers) and test them in a model urban environment. A number of different 3DPV designs are explored and are benchmarked against solar cells that are placed flat on the ground or inclined at 30° to the horizontal. When normalised by their physical footprint area, we find that 3DPV towers can produce as much as 3.05 times as much power in an 'urban environment' as the power generated by a conventionally sited solar cell that is inclined at 30°. Significantly, we also show that light scattered from nearby buildings can enhance the power collected by 3DPV towers by up to 29%. These findings indicate that 3DPV towers present a promising opportunity to generate solar power in complex urban environments.

Keywords: urban energy; power towers; photovoltaics; solar cells; scale model; 3DPV; renewable energy

Academic Editor: James M. Gardner

Received: 8 January 2026
Revised: 10 February 2026
Accepted: 12 February 2026
Published: 20 February 2026

1. Introduction

The rise in global temperature presents a significant threat, with a 1.1 °C increase observed from 2011 to 2020, a process largely attributable to greenhouse gas (GHG) emissions [1]. The energy sector contributes 34% of these emissions, underscoring the urgent need to transition from fossil fuels to alternative energy sources [1]. Urban areas are responsible for around 70% of global energy consumption [2] and are expected to intensify energy demand. Indeed, projections indicate that 70% of the world's population will reside in cities by 2050 [3]. This trend—which is particularly pronounced in developing nations—suggests that rapid urbanisation will drive a 7% annual increase in energy demand [4], a factor that will likely accelerate GHG emissions. Notably, our efforts to decarbonise cities through the electrification of transport, heating, and industry are likely to increase urban electricity demand by a factor of 2.5 times [5]. Notably, the EU [6], the Australian government [7] and the Chinese government [8] have all proposed strategies to reduce energy use in buildings.

The deployment of solar energy within urban environments has been extensively examined through geographic information systems and light detection and ranging models, highlighting a considerable potential for solar energy in urban locations [9,10]. Indeed,

integrating PV panels into the facades of buildings (so-called building integrated photovoltaics) can both facilitate decentralised energy generation and reduce overall energy consumption [11]. However, urban settings pose significant challenges to the successful utilisation of conventional solar installations; here, effects such as shading, pollution, soiling, elevated temperatures, and space constraints are commonplace and all adversely affect PV performance [12,13]. To mitigate these issues, single- and dual-axis tracking systems can enhance solar cell energy output by between 13% and 40% depending on their implementation; however, such devices add significantly to installation costs [14].

It has been found that urban environments (compared to rural areas) are characterised by a higher proportion of diffuse irradiance (due to air pollution) [15] and scattering from buildings [16]. It is known that if we ignore the impacts of air pollution and shading, solar module power output can be overestimated [17], with reductions in direct irradiance potentially decreasing photovoltaic generation by between 15 and 20% [12,18]. While these factors compromise the efficiency of conventional PV systems, they also present an opportunity, as surfaces in urban landscapes (buildings, roads, windows, etc.) may act as secondary light sources which scatter light onto solar installations, an effect that may partly mitigate losses from diminished direct irradiance [19,20].

One way to generate solar energy in an urban landscape is to construct three-dimensional photovoltaic (3DPV) towers. Unlike conventional flat-panel systems, 3DPV towers employ vertical or multi-faceted configurations of solar cells, enabling energy yields that are between 2 and 20 times greater per unit ground area, depending on their specific geometry and design [21]. Such structures can effectively harvest scattered irradiance, as their varied surfaces can collect light incident from multiple directions [22]. This makes 3DPV particularly advantageous in dense urban environments, where the precise geometry of buildings is expected to strongly modify the available amount of reflected light and its angular distribution.

Previous research on this topic has mainly focused on the use of direct and diffuse irradiance in urban PV systems, with the impact of scattered light on the performance of 3DPV towers being largely unexplored [21]. Here, we experimentally quantify the influence of scattered light on the performance of various 3DPV towers within a model urban environment. We do this by building small models of various 3DPV structures and comparing their performance with conventionally situated PV devices. Specifically, we find that when placed in an 'urban environment', 3DPV towers can generate a total absolute power that is up to 3.54 times greater than a single device that is placed on the ground and inclined at 30° towards the horizon. When we normalise the power output of such 3DPV towers by their footprint area, they can generate as much as 3.05 times the power per square metre in an urban environment as conventionally situated PV devices. We explore the incorporation of these models into a model urban landscape, with notable improvements in power generation found (up to 29%) as a result of scattering from the model buildings. These findings highlight the substantial opportunities that exist for practical 3DPV towers in an urban environment.

2. Methods

2.1. Construction of Models

Model 3DPV towers were fabricated from a polylactic acid filament using a 3D printer. Typical models had a height < 10 cm, with polycrystalline silicon solar cells fixed onto their surface. A number of different PV designs were explored, as shown schematically in Figure 1, with photographs of the models shown in Figure 2. As a control, two structures were based on a single solar cell of size 5.25 cm × 2.6 cm = 13.65 cm^2, inclined at 30° to the plane of the surface—here named 'F30' (see Figure 1a), or placed either 'flat' on the test

surface—here named device 'F' (see structure shown in Supplementary Information Figure S1a with a photograph of the structure shown in Figure S2a).

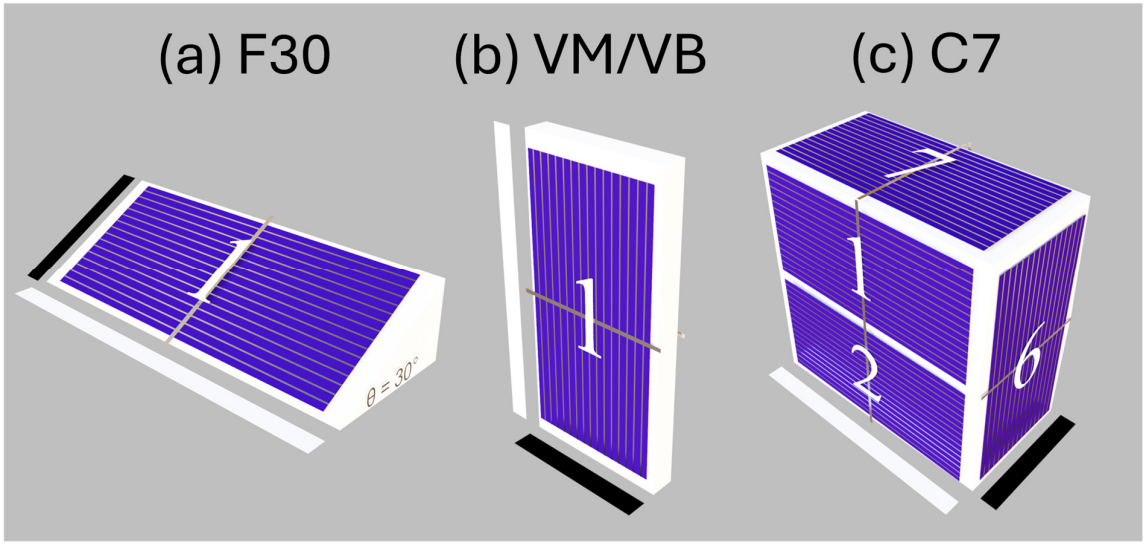

Figure 1. Schematic representations of the most important 3DPV designs tested. Here the blue striped regions correspond to individual solar cells, with the numbers on each solar-cell corresponding to the cell number. Part (**a**) shows a single cell held at 30° to the surface normal ('F30'); part (**b**) shows a vertical structure that is either monofacial ('VM') or bifacial ('VB'). Part (**c**) shows a cuboid structure covered with 7 cells ('C7'). On VB, cell 2 is located on the obscured side and faces Building 2. On C7, cell 3 is opposite cell 6 and faces Building 1 and cells 4 and 5 are opposite cells 1 and 2 and face Building 2. The black and white bars are scale-bars and represent 2.6 cm and 5.25 cm respectively.

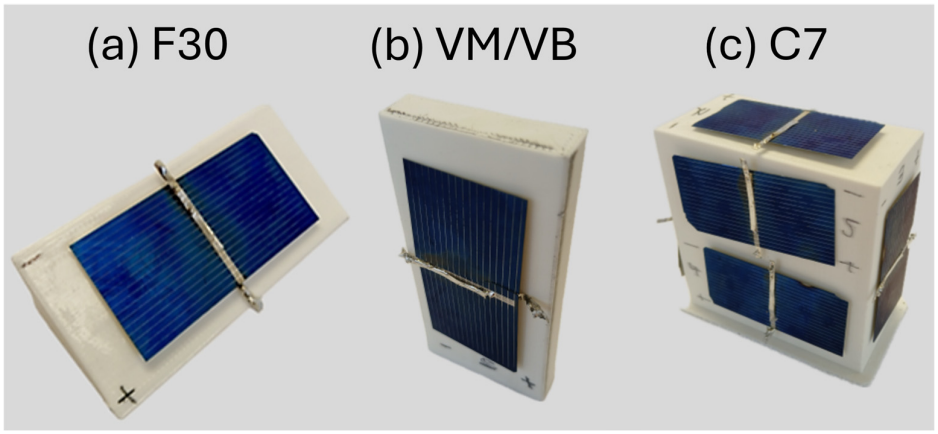

Figure 2. Photographs of the 3DPV designs corresponding to schematics shown in Figure 1. Part (**a**) shows structure F30, part (**b**) corresponds to structure VM and VB, while part (**c**) is C7.

We have explored several 3DPV structures: a vertical monofacial device named 'VM' (see Figure 1b) and a vertical bifacial device named 'VB'. Here, VM consisted of a single solar cell placed at 90° to the test surface. Device VB was based on a similar structure in which two vertical solar cells were placed back-to-back. Two other structures were explored; both of these consisted of a cuboid shape with either 4 or 7 solar cells attached to their various surfaces. We refer to such structures as C4 and C7, with a schematic of C7 shown in Figure 1c. A schematic of C4 is shown in Figure S1b with a photograph of the structure tested in Figure S2b. In each case, the individual cell number is identified in the schematic figure. Each solar cell was connected via wires soldered to its surface and

was tested individually. We estimate that the polycrystalline solar cells used had a power conversion efficiency of between 10 and 15%.

The ability of such structures to harvest light was explored in two contrasting model environments. Firstly, to describe a simplified location without buildings (here referred to as the 'open landscape'), structures were placed on a large, flat surface covered by grey paper having a measured albedo of (0.42 ± 0.1); this material was chosen to replicate the albedo of concrete, and is consistent with the typical urban albedo range of 0.2–0.4 [23]. Here, albedo was measured using a Light Meter LM-3000 app (version 1.9.4) for iOS, with the uncertainty in this value derived from a cosine error (up to 7%) and a systematic measurement error (up to 20%), giving a total uncertainty in albedo of 21%. To explore device performance in a simulated urban environment, a scale model was constructed comprising buildings that were *very loosely* based on the campus of Sheffield University. This is dominated by the Arts Tower building which is 78 m high and is shown in Figure 3a. The model of the campus contained three buildings as can be seen in Figure 3b. Here, Buildings 1, 2 and 3 represent Alfred Denny, the Arts Tower and Dainton respectively. In our model, the height of the model Arts Tower was 27.2 cm which approximately corresponds to 1:287 scale. Again, each building was covered with grey paper having a measured albedo of (0.42 ± 0.1).

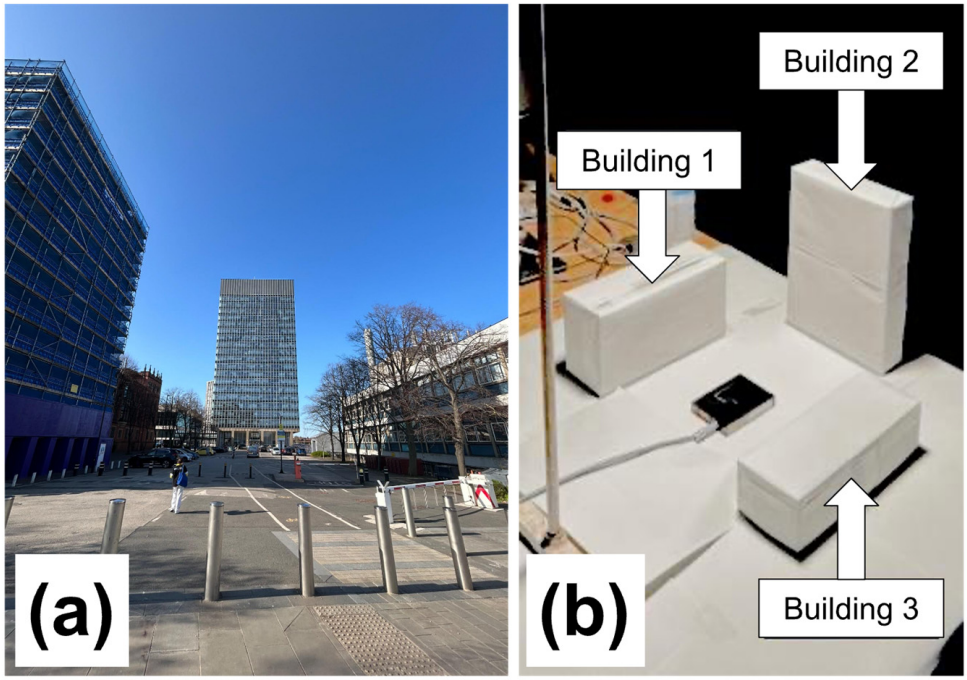

Figure 3. (**a**) The reference environment used for the experiment based on the area surrounding the Arts Tower at The University of Sheffield. Part (**b**) shows the modelled urban environment based on part of the university campus. Here Building 2 corresponds to the Arts Tower visible in the centre of part (**a**).

2.2. Measuring Power Output

To simulate sunlight, a tungsten halogen lamp was placed over the model landscape as shown schematically in Figure 4a,b. Here, the distance between the lamp and the 3DPV model was held fixed at 95 cm, with the measured irradiance falling on the flat surface being approximately 10 mW/cm^2 at a zenith angle of $\theta = 0°$ (as measured using a calibrated power metre). Note that as the lamp had a colour temperature of around 3200 K, it only provided a spectral approximation of sunlight. Nevertheless, we emphasise that it is not the absolute output of devices that is important here; rather, we focus our attention on the relative difference between the different 3DPV towers.

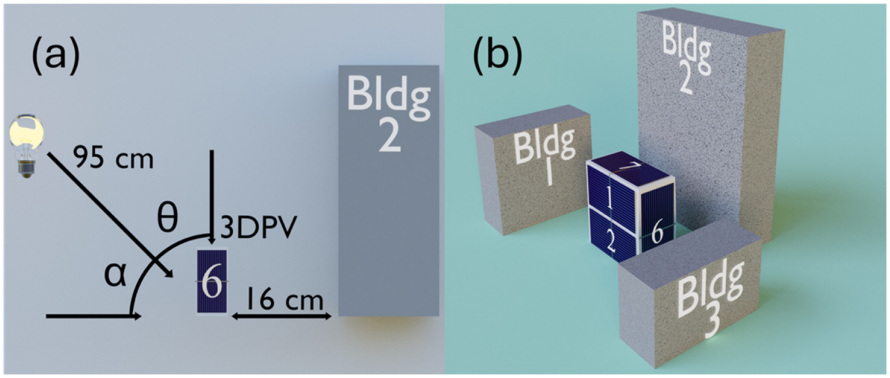

Figure 4. Part (**a**): A schematic of the modelled urban environment. Buildings 1 and 3 are omitted for clarity. The figure defines the zenith angle θ over which measurements were made. Part (**b**): A 3D representation of the modelled urban environment. Here, the dark blue regions correspond to the solar cells that make up the C7 3DPV structure, with the numbers identifying individual sub-cells.

The position and relative angle of the lamp were varied to zenith angles of 0°, 15°, 30°, 45°, 60° and 75°, where the zenith angle is defined as $\theta = 90 - \alpha$. Here α is the altitude angle of the light source, with zenith angles $\theta = 0$ or 90° corresponding to the sun being directly overhead or at the horizon (sunrise/sunset) respectively. In all cases the distance separation between the light source and the place at which the solar cell models were placed remained fixed. This allowed us to approximately model the motion of the sun during the day, although in Sheffield (UK), the zenith angle of the sun at midday in summer is never less than 28–34° degrees.

To test the performance of the various devices, each cell in the 3DPV towers was individually connected to a Keithley source measurement unit (model 2460) which was programmed to record a *JV* curve by sweeping the applied voltage between 0 V and 1 V. To test the performance of the different 3DPV towers, we measured the maximum power generated by each of their component cells at the maximum power point P_{MPP}. The absolute power (P_T) generated by each structure at each angle was determined by summing together the power outputs of all the individual cells in a structure (i.e., $P_T = P_1 + P_2 + \ldots + P_n$, where P_n represents the power generated by the nth cell). We then sum P_T over measured zenith angle to obtain the 3DPV total power output ($\sum P_T$). In a practical implementation of such technology, devices would be connected together in strings to form modules, with by-pass diodes included to account for unwanted shading effects. We have also calculated the power per unit area produced by each structure ($P_A = P_T/A$) where A is the physical footprint of each structure. Again, we can sum P_A over angle to obtain $\sum P_A$.

Note that in structures VM, VB, C4 and C7, the solar cells did not completely extend to the edge of the various surfaces (see Figures 1 and 2). To account for this, we have scaled (reduced) the footprint area used in our calculations to account for this 'dead-space' at the edges of each structure, giving effective areas of C4 and C7 as 6.8 and 13.7 cm^2 respectively. For VM and VB, we assume footprint areas of 2.6 cm^2; here, the thickness of the block on which the devices were fixed contributes significantly to this area. For device F we simply used the physical area of the solar cell (13.6 cm^2), with this being reduced by a factor of cos(30°) to 11.8 cm^2 (i.e., a projection of the device area onto a flat surface) for device F30.

2.3. Errors and Uncertainty

We have attempted to quantify the main sources of error and uncertainty in our measurements. To record device output power, a Keithley source measure unit was used to apply a voltage to the cells and then record output photocurrent. Here, current was determined with a sensitivity of 1 part in 10^{-7} A—a value significantly smaller than the

typical current generated by the individual solar cells, which were often of the order of 50 mA. We believe therefore that errors in the measurement of photocurrent were essentially negligible. We have also explored the repeatability of our measurements (i.e., errors resulting from unintended variation in positioning the 3DPV towers with respect to the light source and model buildings). Here we determine repeatability to be of the order of 0.1%. A further source of uncertainty relates to possible changes in the output power of the tungsten lamp during the course of a measurement. To minimise this effect, the lamp was left to reach its working temperature which was found to take around 10 min. After this, our measurements indicated that the absolute output power of the lamp fluctuated by less than 0.5% over the course of an hour.

A further source of uncertainty related to measurements of the albedo of the grey paper that covered the model buildings that were designed to mimic the albedo of concrete. Here, our albedo measurement had a relatively large uncertainty (0.42 ± 0.1), with this uncertainty likely to propagate into measurements of total power generated by the 3DPV towers. Note that as the 3DPV towers absorbed both direct and scattered light, the importance of any uncertainty in the albedo of the paper affecting the recorded power is expected to be proportionally reduced. Indeed, we estimate that the fractional uncertainty in total power recorded is directly derived from errors in the albedo measurement to be less than 8%. In summary, it is clear that errors in the determination of the albedo of the grey paper and consequently its effectiveness in mimicking the albedo of concrete dominate the overall error associated with our measurements.

3. Results

3.1. Total Power Output of 3DPV Towers as a Function of Zenith Angle

In Figure 5, we plot P_T for F30, VM, VB and C7 as a function of the zenith angle, with measurements recorded in the "open" and "urban" landscapes plotted using light blue and dark-blue lines respectively. Data for structures F and C4 is shown in Figure S3. Figure S4 also plots the power output of each of the individual cells in the different 3DPV towers and discusses the general trends observed.

As might be expected, structure C7 generates the highest absolute power in both environments over all angles as a direct consequence of its increased active area (and greatest number of solar cells). Indeed, its generation yield at a zenith angle of 0 degrees (i.e., 'sun' overhead) is significantly larger than all other structures. For example, in an open environment, it generates 2.5 times more power than F30, 7.9 times more than VM and 4.4 times more than VB. We find that the power generated by VM, VB and C7 all increase with increasing zenith angles up to around 60°, after which this either reduces or saturates—an effect resulting from the vertical presentation of the solar cells on these structures. In contrast, the power generated by structure F30 declines with zenith angles beyond 15° as this device subtends a smaller solid angle as the "sun" approaches the horizon.

3.2. Comparing Power Output in Urban vs. Open Environments

Figure 6a compares P_T for F30, VM, VB and C7 summed over all measured zenith angles in open and urban environments (ΣP_T). Clearly, structure C7 out-performed all other structures in terms of overall (total) power output, as it had the largest active area. If we compare its total power generation in the urban environment with that of the other structures, we find it generates 3.54, 3.81 and 2.83 times as much as F30, VM and VB respectively. As might be expected, we find that the power generated by structures that have building-facing cells (i.e., VB and C7) improve substantially when they are placed in an urban setting, indicating that a substantial amount of scattered light can be harvested from the surrounding buildings. Indeed, this enhancement in an urban environment is

particularly pronounced in device C7, where an enhancement in total power output of approximately 29% is recorded. The effect of scattered illumination in the urban environment is also apparent if we compare the power generated by structure F30 with VB (see Figure 5a,c). For example, in the open environment at $\theta = 15°$, structure F30 generated 40% more power compared to VB. However, in the urban environment, the power generated by VB and F30 at $\theta = 15°$ is more similar (to within 7%).

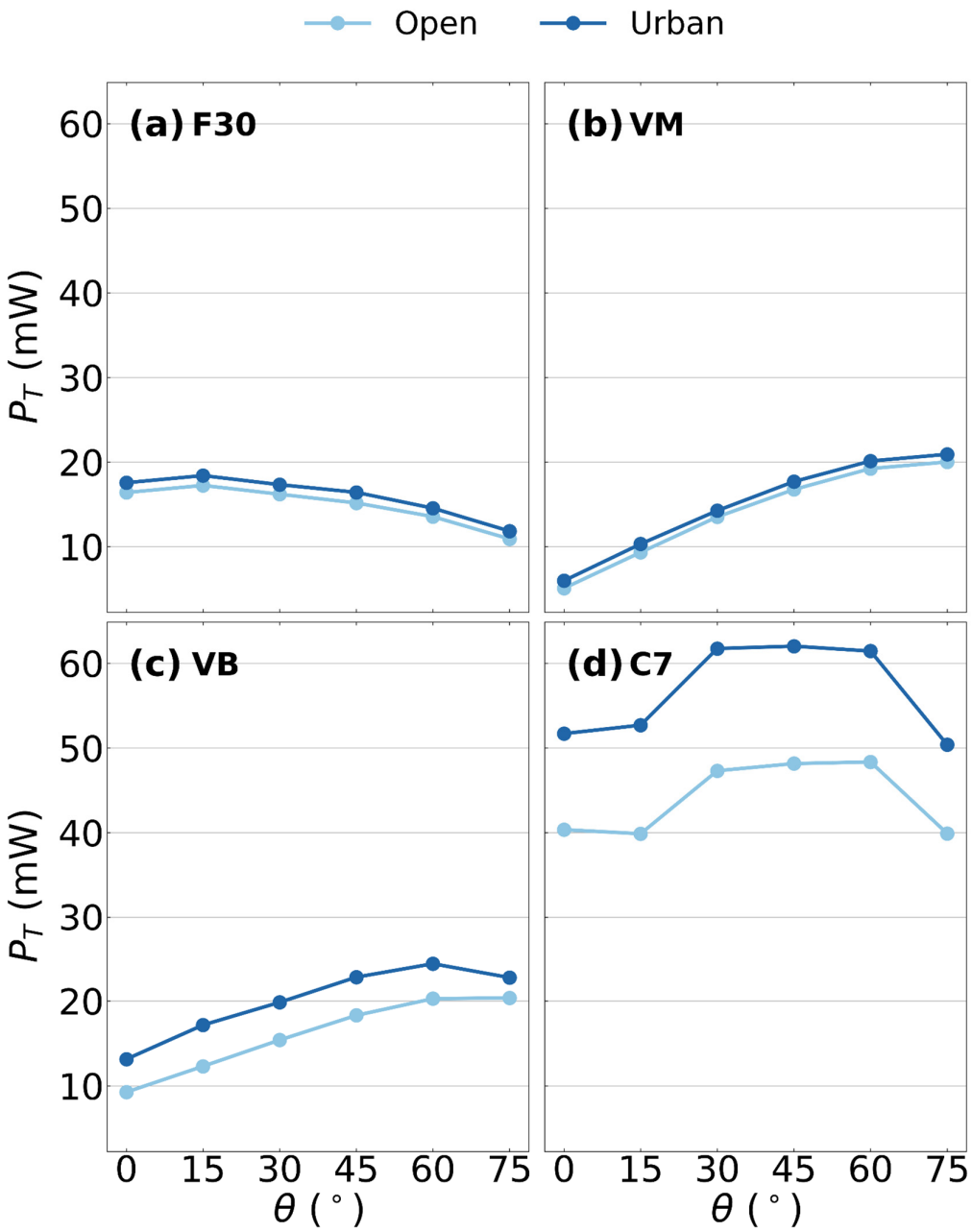

Figure 5. The total power generated by each structure as a function of zenith angle (θ). This is shown for both the open and urban environment. Data is shown for F30 in part (**a**), for VM in part (**b**), for VB in part (**c**) and for C7 in part (**d**).

It is interesting to compare the output summed over all measured zenith-angles for each structure when normalised by its physical footprint area (ΣP_A) as shown in Figure 6b. Here we again show data recorded in open and urban environments. The footprint-corrected power output is clearly an important parameter, as it is a measure of how effectively land space would be utilised in an urban environment. If we compare

the output of C7 with device F30, we find that ΣP_A is 2.54 times larger respectively when measured in the open environment and 3.05 times larger in the urban environment. This clearly demonstrates the gains that can be obtained in power harvesting by utilising 3DPV towers over conventionally mounted devices. It can also be seen that structures VM and VB achieved the highest values of P_A as the footprint area of such structures can be made very small and is intrinsically limited by the thickness of the solar cell itself. Clearly, however, there is a limit to which this area could be reduced in practice; this would be ultimately limited by the stability of the frame on which the solar cell was mounted. Note however that while the area normalised output from structures VM and VB is high, their total power output compared to C7 is relatively reduced as a result of their smaller active surface area. For completeness, we also show comparable data including structures F and C4 in Figure S5.

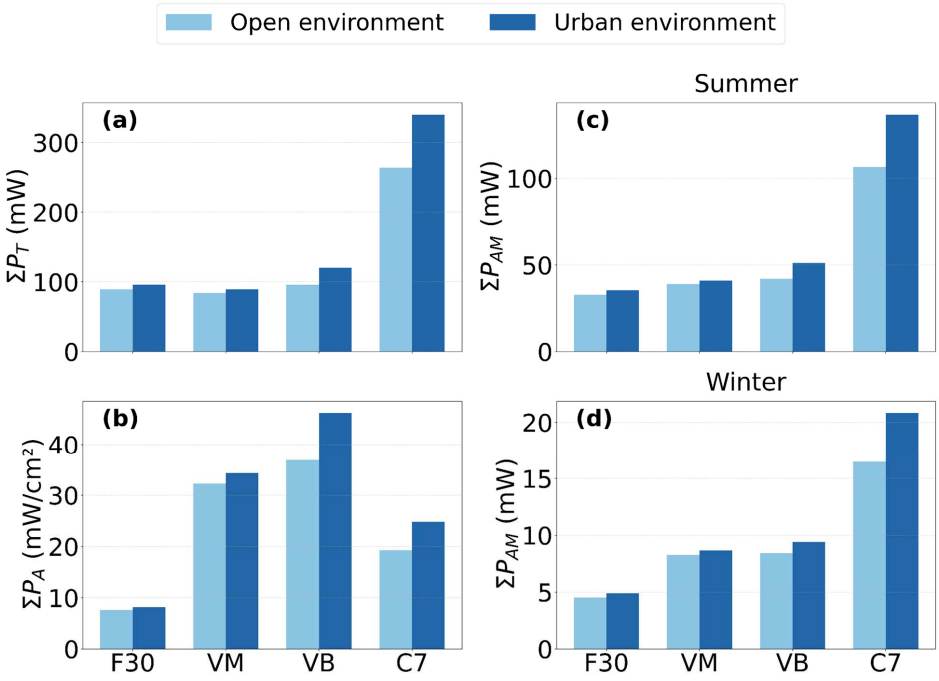

Figure 6. Part (**a**) shows the total power generated by each structure integrated over the complete range of measured zenith angles 0-75° (ΣP_T). Part (**b**) shows the power generated by each structure as shown in part (**a**); however, this is now normalised by the footprint area of each structure (ΣP_A). Parts (**c**,**d**) plot the calculated air mass corrected total power output (ΣP_{AM}) of each structure. This assumes structures are located in Sheffield with power generation corrected for the effects of atmospheric absorption. To simulate summer months, total power is summed over zenith angles 30°, 45°, 60° and 75° (see part (**c**)). To simulate winter months (see part (**d**)) we simply use the power measured at 75°.

3.3. Comparing Total Power Output for 3DPV in Sheffield: Summer vs. Winter

We now estimate the relative power that could be generated by such structures if they were situated at a latitude commensurate with the city of Sheffield, U.K. (53.38° North). Indeed, as we describe below, we use our experimental data to compare the predicted performance of the different structures in the summer and winter months, and we take account of the effects of absorption of sunlight by the atmosphere. To do this, we firstly note that the maximum zenith angle of the sun in Sheffield is approximately 31° at midsummer and 77° in midwinter. To describe summertime, we sum the measured power output for the various cells measured at 30°, 45°, 60° and 75°. Here we assume an idealised day length where the sun's trajectory is sampled at the four discrete zenith angles, with an equal dwell time at each position. To describe the winter, we simply use the power measured at 75°. Note that we did not record power at θ = 90°; at this very high zenith angle the sun would

be very likely obscured by objects in the environment—this effect would be particularly significant in an urban environment.

To account for the effects of absorption of sunlight in the atmosphere, we use the empirical Kasten–Young formula [24] to calculate the relative optical air mass (m) as a function of the Sun's zenith angle θ. From this, we then calculate the expected transmission (τ) by the atmosphere as a function of m, using $\tau(m) = 0.7^{m^{0.678}}$, with this approach based on the model of Meinel and Meinel [25]. Using this, we obtain atmospheric transmission values $\tau(\theta)$ = 0.675, 0.637, 0.566 and 0.413 at θ = 30°, 45°, 60° and 75° respectively. This factor is then used to correct the measured 3DPV output power (P_T) at each angle to obtain an air mass corrected power output (P_{AM}) where $P_{AM} = \tau(\theta)\ P_T$. Finally, these values were summed over angle (as described above) to obtain a total air mass corrected power output ($\sum P_{AM}$). Note that we do not correct for any changes in the spectral distribution of light as a function of position in the sky.

Figure 6c,d plot $\sum P_{AM}$ generated by each structure in the "summer" and "winter". It is notable that in all cases the power produced by the various devices in winter is reduced by between 4.7 (VM) and 7.2 (F30) times (urban data). Notably, this reduction is most significant in structure F30 as might be expected as such devices are much less able to harvest light as the "sun" is low on the horizon; indeed, we find that the power output of F30 in winter is only 14% of that generated in the summer. This value is consistent with the measured power output of solar cell located at a latitude corresponding to Sheffield (UK), where it has been found that the total daily yield of a solar cell in the winter can drop to as low as 10–15% of its summer daily total [26]. We also find that in the winter, the output from VM and VB is around 1.8 and 1.9 times greater than that produced by F30 due to their favourable vertical orientation, although their relative output is only 21% (VM) and 18% (VB) of their production during "summer" months.

4. Discussion

It is clear that there are opportunities to enhance the collection efficiency of 3DPV towers by harvesting light scattered from nearby buildings; however, this is likely to be intrinsically limited by building size, shape, proximity and albedo. Indeed, we find a variation in power generated by the different cells in our 3DPV towers—a result that derives from the physical area of the different buildings in our model and their relative location with respect to the 3DPV tower. It is clear however that the models constructed represent a significant simplification of a practical urban environment, as they do not include vegetation, materials and surfaces with a lower albedo (e.g., black tarmac) and glass surfaces that generate highly directional reflection of sunlight. Our experiment, therefore, is clearly biased towards diffuse scattering, rather than specular reflection. To address this, it would be necessary to create models having increased sophistication, or we suggest designing and building full-sized structures that can be tested under real-world conditions. This will allow effects such as the effects of day-length, season and changes in spectral quality of scattered light to be included in a more comprehensive way. Indeed, although we include some effects of absorption by the atmosphere in our calculations, we do not include spectral changes as might be practically expected at high solar zenith angles which are likely to be important.

Our experiments indicate that harvesting scattered light in cities should be an effective strategy to enhance the power generated by a 3DPV tower. However, whether such structures would fit easily into the landscape is a matter of debate. Clearly there are plenty of possible objections to their practical implementation, as they may act as obstacles to pedestrians, become targets for graffiti or vandalism, or have a negative aesthetic impact in a sensitive urban environment. We also note that if building integrated PV becomes

very widespread in cities, then there is likely to be less scattered light available to be harvested; however, this prospect is currently a long way off. It is clear therefore that 3DPV towers need to fit into an urban landscape in a way that provides a practical benefit to the local inhabitants, rather than being an incumbrance. We suggest that the optimum implementation of such structures will likely come when they in fact have a dual purpose—for example, also acting as small buildings, kiosks, bus shelters, information points, etc. We believe such issues represent an exciting challenge for building designers, architects and urban planners.

5. Conclusions

We have constructed physical models of three-dimensional solar cell towers and have tested their performance in a model urban environment, loosely based on the campus at the University of Sheffield. We have recorded the power generated by the different cells within such towers and have compared the output of our structures per unit area of land occupied with a solar cell that is conventionally mounted at an angle of 30° degrees with respect to the horizon. We show that a relatively simple device consisting of seven solar cells mounted on a box frame (C7) can generate a power per unit area of land that is 2.54 times larger than a single conventionally mounted solar cell angled at 30° to the horizontal (F30), with this power being further enhanced to 3.05 times when light scattered of neighbouring buildings is included.

We have also compared the power output of the various 3DPV towers when located at northern latitudes in both the summer and the winter and find as expected the power generated is reduced by over an order of magnitude during winter months; however, such effects are relatively less prominent in structures in which solar cells are oriented vertically. Our work therefore suggests that the construction of 3DPV towers in space-constrained environments is likely to be a promising strategy to provide solar power to local users, and that such energy may be enhanced by the proximity of nearby buildings.

Supplementary Materials: The following supporting information can be downloaded at: https://www.mdpi.com/article/10.3390/en19041077/s1, Figure S1: Schematic representations of two additional PV designs tested; Figure S2: Photographs of two additional 3DPV designs tested; Figure S3: The power generated by structures F and C4 as a function of zenith angle; Figure S4: The power generated by the different structures distributed across individual cells; Figure S5: Total power generated by the different structures., including data for 'F' and 'C4'.

Author Contributions: Formal analysis, J.B.; Investigation, J.B.; Writing—original draft, J.B.; Writing—review & editing, T.T. and D.G.L.; Visualization, T.T.; Supervision, D.G.L.; Project administration, D.G.L. All authors have read and agreed to the published version of the manuscript.

Funding: This research was partly funded by the Engineering and Physical Sciences Research Council (EPSRC) grant EP/V027131/1 (High-efficiency flexible and scalable halide-perovskite solar modules).

Data Availability Statement: The raw data supporting the conclusions of this article will be made available by the authors on request.

Conflicts of Interest: D.G.L. is co-director of the company Ossila Ltd. which retails materials used in photovoltaic research.

References

1. Intergovernmental Panel on Climate Change (IPCC). *IPCC Climate Change 2023: Synthesis Report. Contribution of Working Groups I, II and III to the Sixth Assessment Report of the Intergovernmental Panel on Climate Change*; Intergovernmental Panel on Climate Change (IPCC): Geneva, Switzerland, 2023. [CrossRef]
2. Sethi, M.; Creutzig, F. Leaders or laggards in climate action? Assessing GHG trends and mitigation targets of global megacities. *PLoS Clim.* **2023**, *2*, e0000113. [CrossRef]

3. World Bank. Urban Development Overview. 2022. Available online: https://www.worldbank.org/en/topic/urbandevelopment/overview/ (accessed on 26 February 2025).
4. UN-Habitat. World Cities Report 2024: Charting a Better Urban Future. United Nations Human Settlements Programme. 2024. Available online: https://unhabitat.org/wcr/ (accessed on 26 February 2025).
5. International Energy Agency. *Empowering Urban Energy Transitions*; IEA: Singapore, 2024. Available online: https://www.iea.org/reports/empowering-urban-energy-transitions/ (accessed on 24 February 2025).
6. Available online: http://data.europa.eu/eli/dir/2024/1275/oj (accessed on 1 February 2025).
7. Australian Government. *Built Environment Sector Plan*; Australian Government: Canberra, Australia, 2025. ISBN 978-1-923278-28-8.
8. Available online: https://chinaenergyportal.org/en/2024-2025-energy-conservation-and-carbon-reduction-action-plan/ (accessed on 1 February 2025).
9. Fakhraian, E.; Alier, M.; Valls Dalmau, F.; Nameni, A.; Casañ Guerrero, M.J. Theurban rooftop photovoltaic potential determination. *Sustainability* **2021**, *13*, 7447. [CrossRef]
10. Zhou, Y.; Verkou, M.; Zeman, M.; Ziar, H.; Isabella, O. A Comprehensive Workflow for High Resolution 3D Solar Photovoltaic Potential Mapping in Dense Urban Environment: A Case Study on Campus of Delft University of Technology. *Sol. RRL* **2022**, *6*, 2100478. [CrossRef]
11. Zhang, T.; Wang, M.; Yang, H. A Review of the Energy Performance and Life-Cycle Assessment of Building-Integrated Photovoltaic (BIPV) Systems. *Energies* **2018**, *11*, e3157. [CrossRef]
12. Sailor, D.; Anand, J.; King, R. Photovoltaics in the built environment: A critical review. *Energy Build.* **2021**, *253*, e111479. [CrossRef]
13. Etukudoh, E.A.; Nwokediegwu, Z.Q.S.; Umoh, A.A.; Ibekwe, K.I.; Ilojianya, V.I.; Adefemi, A. Solar power integration in Urban areas: A review of design innovations and efficiency enhancements. *World J. Adv. Res. Rev.* **2024**, *21*, 1383–1394. [CrossRef]
14. Alomar, O.R.; Ali, O.M.; Ali, B.M.; Qader, V.S.; Ali, O.M. Energy, exergy, economical and environmental analysis of photovoltaic solar panel for fixed, single and dual axis tracking systems: An experimental and theoretical study. *Case Stud. Therm. Eng.* **2023**, *51*, e103635. [CrossRef]
15. Zhang, X.; Zhang, M.; Cui, Y.; He, Y. Estimation of Daily Ground-Received Global Solar Radiation Using Air Pollutant Data. *Front. Public Health* **2022**, *10*, e860107. [CrossRef] [PubMed]
16. Zhu, R.; Cheng, C.; Santi, P.; Chen, M.; Zhang, X.; Mazzarello, M.; Wong, M.S.; Ratti, C. Optimization of photovoltaic provision in a three-dimensional city using real-time electricity demand. *Appl. Energy* **2022**, *316*, e119042. [CrossRef]
17. Arias-Rosales, A.; LeDuc, P.R. Urban solar harvesting: The importance of diffuse shadows in complex environments. *Renew. Sustain. Energy Rev.* **2023**, *175*, e113155. [CrossRef]
18. Huld, T.; Gracia Amillo, A.M. Estimating PV Module Performance over Large Geographical Regions: The Role of Irradiance, Air Temperature, Wind Speed and Solar Spectrum. *Energies* **2015**, *8*, 5159–5181. [CrossRef]
19. Boccalatte, A.; Fossa, M.; Menézo, C. Best arrangement of BIPV surfaces for future NZEB districts while considering urban heat island effects and the reduction of reflected radiation from solar façades. *Renew. Energy* **2020**, *160*, 686–703. [CrossRef]
20. Badran, G.; Dhimish, M. Comprehensive study on the efficiency of vertical bifacial photovoltaic systems: A UK case study. *Sci. Rep.* **2024**, *14*, e18380. [CrossRef] [PubMed]
21. Bernardi, M.; Ferralis, N.; Wan, J.H.; Villalon, R.; Grossman, J.C. Solar energy generation in three dimensions. *Energy Environ. Sci.* **2012**, *5*, 6880–6884. [CrossRef]
22. Myers, B.; Bernardi, M.; Grossman, J.C. Three-dimensional photovoltaics. *Appl. Phys. Lett.* **2010**, *96*, e071902. [CrossRef]
23. Salvati, A.; Kolokotroni, M.; Kotopouleas, A.; Watkins, R.; Giridharan, R.; Nikolopoulou, M. Impact of reflective materials on urban canyon albedo, outdoor and indoor microclimates. *Build Environ.* **2022**, *207*, e108459. [CrossRef]
24. Kasten, F.; Young, A.T. Revised optical air mass tables and approximation formula. *Appl. Opt.* **1989**, *28*, 4735–4738. [CrossRef] [PubMed]
25. Meinel, A.B.; Meinel, M.P. *Applied Solar Energy*; Addison Wesley Publishing Co.: Boston, MA, USA, 1976.
26. Available online: https://www.solar.sheffield.ac.uk/pvlive/ (accessed on 1 February 2025).